The Protein Journal (2021) 40:68–77
https://doi.org/10.1007/s10930-020-09950-9

c.1898C>G/p.Ser633Trp Mutation in Alpha-L-Iduronidase: Clinical and Structural Implications

Iliana Peña-Gomar[1] · José L. Jiménez-Mariscal[1] · Magdalena Cerón[2] · Jorge Rosas-Trigueros[3] · Cesar A. Reyes-López[4]

Accepted: 10 December 2020 / Published online: 2 January 2021

Abstract
Mucopolysaccharidosis type I is a rare autosomal recessive genetic disease caused by deficient activity of α-L-iduronidase. As a consequence of low or absent activity of this enzyme, glycosaminoglycans accumulate in the lysosomal compartments of multiple cell types throughout the body. Mucopolysaccharidosis type I has been classified into 3 clinical subtypes, ranging from a severe Hurler form to the more attenuated Hurler–Scheie and Scheie phenotypes. Over 200 gene variants causing the various forms of mucopolysaccharidosis type I have been reported. DNA isolated from dried blood spot was used to sequencing of all exons of the *IDUA* gene from a patient with a clinical phenotype of severe mucopolysaccharidosis type I syndrome. Enzyme activity of α-L-iduronidase was quantified by fluorimetric assay. Additionally, a molecular dynamics simulation approach was used to determine the effect of the Ser633Trp mutation on the structure and dynamics of the α-L-iduronidase. The DNA sequencing analysis and enzymatic activity shows a c.1898C>G mutation associated a patient with a homozygous state and α-L-iduronidase activity of 0.24 µmol/L/h, respectively. The molecular dynamics simulation analysis shows that the p.Ser633Trp mutation on the α-L-iduronidase affect significant the temporal and spatial properties of the different structural loops, the N-glycan attached to Asn372 and amino acid residues around the catalytic site of this enzyme. Low enzymatic activity observed for p.Ser633Trp variant of the α-L-iduronidase seems to lead to severe mucopolysaccharidosis type I phenotype, possibly associated with a perturbation of the structural dynamics in regions of the enzyme close to the active site.

Keywords Mucopolysaccharidosis · Alpha-L-iduronidase mutation · Hurler · Structural dynamics

1 Introduction

Mucopolysaccharidosis type I (MPS I) is a rare autosomal recessive genetic disease caused by deficient activity of the α-L-iduronidase (IDUA; EC 3.2.1.76), enzyme that hydrolyzes the terminal α-L-iduronic acid residues of the glycosaminoglycans (GAGs) dermatan sulfate and of heparan sulfate [1]. As a consequence of low or absent activity of the mutant enzyme, the GAGs accumulate in the lysosomal compartments of multiple cell types throughout the body, resulting in a progressive and multisystem dysfunction. Clinical findings usually include coarse facial features, dysostosis multiplex, short stature, corneal clouding, hepatosplenomegaly, umbilical hernias, joint contractures, failure to thrive, and intellectual disability [2]. There is a wide spectrum of symptoms, ranging from a severe Hurler form (OMIM#607015) to the more attenuated Hurler–Scheie (OMIM#607015) and Scheie (OMIM#67016) phenotypes.

✉ Cesar A. Reyes-López
careyes@ipn.mx

1 Hospital Pediátrico Tacubaya, Secretaría de Salud, Ciudad de México, Mexico

2 Clínica de Enfermedades Lisosomales, Hospital Infantil de México Federico Gómez, Ciudad de México, Mexico

3 Laboratorio Transdisciplinario de Investigación en Sistemas Evolutivos, ESCOM, Instituto Politécnico Nacional, Ciudad de México, Mexico

4 Laboratorio de Bioquímica Estructural, Sección de Estudios de Posgrado E Investigación, ENMyH, SEPI-ENMyH, Instituto Politécnico Nacional., Guillermo Massieu Helguera, No. 239, Fracc. "La Escalera", Ticomán, C.P. 07320 Ciudad de México, Mexico

The gene encoding IDUA is localized on chromosome 4p16.3, contains 14 exons [3], and encodes a precursor protein of 653 amino acids which is glycosylated and processed to a mature form of 626 residues [4].

There are more than 200 variants described in the *IDUA* gene that can cause MPS I; the majority are missense variants [5]. This high degree of molecular heterogeneity is thought to reflect the wide clinical variability.

An analysis of the crystallographic structure reveals that IDUA has three prominent domains: a TIM barrel domain containing the active site residues (residues 42-396), a β-sandwich domain containing the N-terminus of the enzyme and containing the first β-strand (residues 27-42 and 397-541), and a third domain that resembles the fold of a Type III Fibronectin-like/Ig-like domain and consists of the C-terminal residues of the enzyme (residues 546-642) [6, 7]. The catalytic site of IDUA is structured by highly conserved amino acid residues, 5 with a substrate binding function (H91, Q181, K264, D349 and R363) and 2 catalytic residues, D182 as a proton donor, and D299 as a nucleophile group. A two-step Koshland double-displacement mechanism, yielding a covalent enzyme–substrate intermediate, is formed through catalysis [8].

Missense variants associated with severe or intermediate-severe MPS I phenotypes have been identified mainly in the TIM-barrel domain (approximately 75%). In the β-sandwich domain, there are around 20% missense variants and only 5% in the Type III Fibronectin-like domain [9]. Regarding the missense variants reported in the Type III Fibronectin-like domain, the variants p.*654Cys, that generates a 38-amino acid-extended protein, p.Val620Phe and p.Trp626Arg have been associated with a severe (Hurler) phenotype, and the variants p.Arg619Gly and Ser633Leu have been associated with a more attenuated Hurler–Scheie or Scheie phenotype [10]. In this same domain, some nonsense variants incorporating an early stop codon generate mostly a Hurler phenotype (observed in Arg619 and Arg621 positions) [11]. The contribution of the Type III fibronectin-like domain in IDUA enzymatic activity and how mutations in this region of the IDUA can affect the catalysis of the enzyme have not been fully understood.

Here, we describe the case of one male patient who presents an IDUA variant c.1898C>G/p.Ser633Trp which seems to lead to the severe phenotype, in contrast to a previously reported variant at the same nucleotide and amino acid position, identified as c.1898C>T/p.Ser633Leu, that has been found in patients with an attenuated phenotype [12]. Additionally, here we use a molecular dynamics approach to determine the influence of the Ser633Trp mutation on the structural dynamics of the α-L-iduronidase and to better understand the contribution of the Type III fibronectin-like domain to the function of IDUA.

2 Materials and Methods

This study was made after obtaining appropriate informed consent, and the Ethical Committee of Pediatric Hospital of Tacubaya approved this study (code number: 309-010-10-17, April 15, 2017).

2.1 Clinical Findings

A 20-month-old male patient is the first son of healthy non-consanguineous parents with an unremarkable family history. He was born with neonatal complications, late in crying and breathing, hyporeactive Apgar 5/8 Silverman-Anderson 3/2. Since 3 months of life, he manifested snoring and noisy breathing. At the age of 8 months, he presented sleep apnea, upper airway obstruction, episodes of breathing cessation and cyanosis. He had a history of frequent upper airway infections. He was referred to geneticist for facial dysmorphic features and short stature.

2.2 Biochemical and Molecular Analysis

IDUA enzymatic analysis was carried out by Sanofi-Genzyme (México) on dried blood spot (DBS) samples collected from the patient and his parents. Fluorescent 4-methylumbelliferyl (4MU)-α-L-iduronide was used as substrate and enzymatic activities were expressed as micromoles of substrate hydrolyzed per liter of blood per hour (μmol/L/h).

Molecular diagnosis was performed by sequencing all exons of the IDUA gene at Sanofi-Genzyme (México). DNA was isolated from DBS samples collected from the patient and his parents and PCR- amplified with short flanking intronic sequences. This was followed by conventional Sanger sequencing using Gene Analyzer 3730 (Applied Biosystem).

2.3 Molecular Dynamics Analysis

For molecular dynamics simulations (MD), the suite GROMACS [13] version 5.1 was used and the CHARMM-GUI Input Generator [14] was employed to protein and carbohydrates force field (CHARMM36) and to Ser633Leu and Ser633Trp mutation constructions; the time step was 2.0 fs and hydrogen virtual sites were employed. For the simulation of the wild-type (WT) and mutant enzymes, the PDB 3W81 structure was used. Each monomeric structure was independently solvated in a dodecahedral box with its nearest edge 1.0 nm away from the protein, and TIP3P explicit water model was used for all simulations. Chloride ions were added to neutralize each system, and all electrostatic interactions were calculated within the Particle

Mesh Ewald (PME) approach. Energy minimization was performed using the steepest descent algorithm for 5000 steps. Then, a restrained MD simulation of 1000 ps was performed to allow the solvent to relax; the peptide atoms were harmonically restrained to their position in the crystal with a force constant of 1000 kJ/mol/nm^2. All simulations were performed at 300 K and 1 atm pressure. The free MD run was carried out for 50 ns with the same pressure- and temperature-coupling constants as the restrained run. All steps of the simulations were performed using periodic boundary conditions.

A post-simulation analysis of the principal components (PCA) was performed using GROMACS, employing the modules covar and anaeig for the calculation and diagonalization of the covariance matrix and analysis of the eigenvectors, respectively. The principal components (PCs) were obtained from mapping the C-alpha atoms of all the simulated trajectories of WT, Ser633Leu, and Ser633Trp IDUA variants. The eigenvectors and the corresponding eigenvalues were produced by the diagonalization of the covariance matrix. Eigenvectors stand for the directions of atomic motions which are independent of each other in the multidimensional space, while the eigenvalues describe the corresponding magnitude. The frequency of sampling from all MD simulations was set to 100 ps. To extract distinct conformational states of the structures, the principal components PC1 and PC2 were used. The GROMACS sham module was used to compute the probability sampling (u) landscape in the PC1–PC2 conformational space from the simulated trajectories identified by the anaeig module.

3 Results and Discussion

3.1 *Clinical Features of Patient with c.1898C>G/p.Ser633Trp IDUA Mutation Corresponding with Hurler Phenotype*

At clinical examination, the patient had a short stature (78 cm of height; − 3 S.D.), 10 kg of weight (− 3 S.D.) and a head circumference of 50.5 cm (> 90th percentile). A detailed clinical and radiological examination was carried out, which showed coarse facial features, the skull with scaphocephaly, a bulging frontal bone (Fig. 1A), mild corneal clouding, a depressed nasal bridge, a wide nose and anteverted nares, nasal congestion, long philtrum, thick lips, small and spaced teeth (Fig. 1B), enlarged tongue, low set ears (Fig. 1C), short neck and trunk, gibbus deformity, protruding abdomen, umbilical hernia (Fig. 1D), the liver edge was palpated 2 cm below the right costal margin, blue cutaneous pigmentation with dorsal distribution (Fig. 1E), limited extension of the arms and small joints (Fig. 1F), and claw hands (Fig. 1G). He presented global developmental delay, no ability yet to walk and speak at the age of 20 months.

A skeletal radiologic analysis showed evidence of dysostosis multiplex. Scoliosis was evident (Fig. 2A), broadening of ribs bilaterally (Fig. 2B), lumbar gibbus with vertebral hypoplasia (Fig. 2C), scaphocephaly (Fig. 2C), hand bullet-shaped phalanges and widened metacarpals pointed proximally (Fig. 2D), widened diaphysis and cortical thinning of long bones (Fig. 2D and G), and pelvis with rounded or flared iliac wings (Fig. 2A and D). Clinical features agree with a severe phenotype of MPS I [2]. The patient started on enzymatic replacement therapy at 2 years of age.

4 Molecular and Enzymatic Analysis

4.1 *c.1898C>G/p.Ser633Trp Variant Yields an IDUA with Low Enzymatic Activity*

The DNA sequencing analysis and enzymatic activity shows a c.1898C>G variant associated a patient with a homozygous state and IDUA activity of 0.24 µmol/L/h, respectively. Enzymatic IDUA activity was 10 times less than the reference minimum level of this enzyme (2.02–16.10 µmol/L/h). Clinical, biochemical and molecular evidence should arouse suspicion of a Hurler MPS I phenotype. The residual enzymatic activity observed in the Ser633Trp variant, which would not be expected to cause a severe phenotype, may be due to the use of a synthetic substrate, which could sufficiently evaluate the impact of the variants on the disposition of the residues that make up the active site of enzyme, but might lack sensitivity to assess perturbations in regions of the enzyme involved in binding to the natural substrate that are farthest from the active site.

Sequence analysis of parental genomic DNA showed that both parents are heterozygous for c.1898C>G variant, with no clinical phenotype of MPS I. Enzymatic IDUA activity was 1.29 µmol/L/h and 3.25 µmol/L/h for the father and the mother, respectively. These levels were 5.4 and 13.5 higher than the ones observed in the patient, respectively. The low enzyme activity observed in the father, which would be expected to be greater because he is a heterozygous with a normal allele, could be explained by a condition known as pseudodeficiency, in which clinically normal individuals shows levels of enzyme activity below the normal levels [15].

Undetectable enzymatic activity for the same variant of IDUA was recently reported in patients with clinical diagnosis of MPS I [16]. Nevertheless, the consequences of this missense variant in the MPS I phenotype have not been previously well defined.

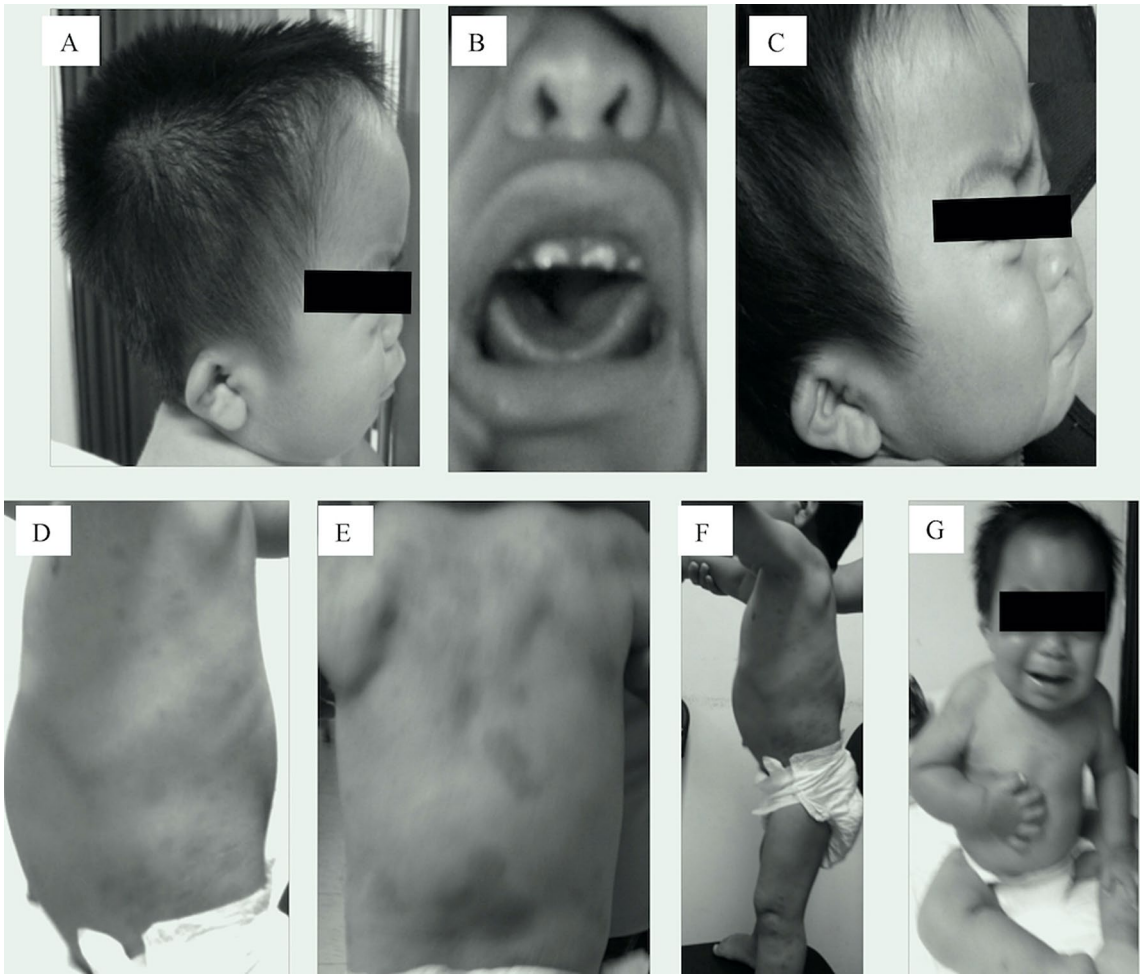

Fig. 1 Clinical features. A 20 month-old boy with Mucopolysaccharidosis I. **A** Scaphocephaly with frontal bossing. **B** Coarse facial features, thick lips, spacing and irregular shaped teeth. **C** Low set ears. **D** Protuberant abdomen, umbilical hernia and thoracolumbar kyphosis. **E** Mongolia spots. **F** Limited extension of the arms. **G** Claw hands

Interestingly, the variant p.Ser633Leu reported in a Pakistani patient generated an attenuated (Scheie) phenotype when it was present in the homozygous form, or a severe (Hurler) phenotype (in a Thai patient) when it was found in combination with an p.Arg75Thr variant [12, 17]. This leucine mutant, expressed in COS-7 cells (a cell line derived from the kidney of the African Green Monkey), showed an in vitro IDUA enzymatic activity of 5.4 nmol/h/mg cell protein, 16 times less than obtained for the wild-type enzyme expressed in the same system. IDUA folding, protein stability, or a glycosylation profile in this expression system could explain, at least partially, the reason why this mutant with significantly decreased in vitro activity does not generate a severe phenotype of the disease in carrier patients.

5 Structural Dynamics Analysis

5.1 Ser633Leu and Ser633Trp Mutations Do Not Modify the Global IDUA Structure

To our knowledge, Ser633Trp is the fourth missense mutation reported in the Type III fibronectin-like domain of IDUA that causes a severe (Hurler) phenotype.

The molecular dynamic simulations performed in this study allow us to illustrate the effect of the Ser633Trp mutations on the molecular dynamics of the human α-L-Iduronidase, and the results were compared with those obtained for the wild-type structure (PDB: 3W81) and the Ser633Leu variant model.

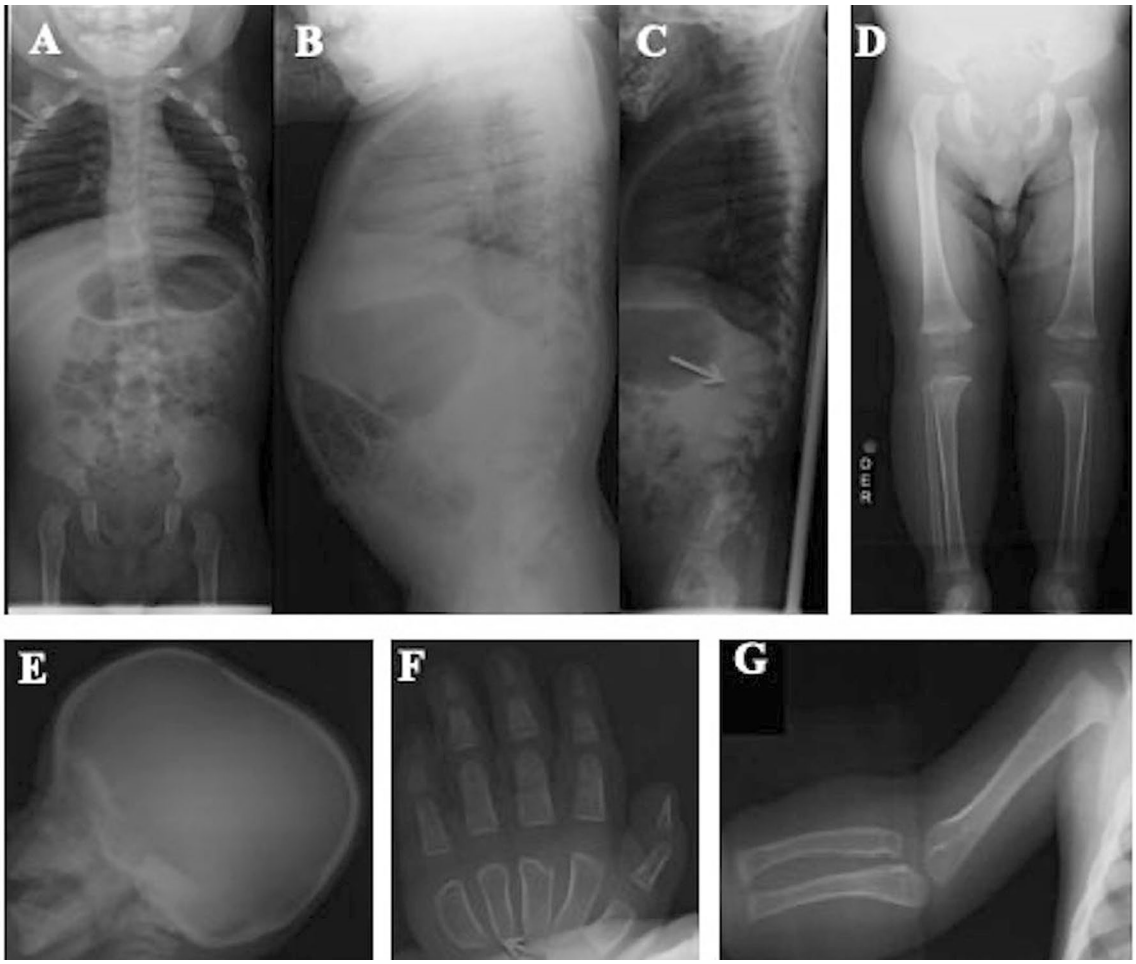

Fig. 2 Radiological analysis. Skeletal X-rays showed evidence of dysostosis multiplex. **A** and **B** Frontal and lateral chest radiograph demonstrates scoliosis and broadening of the ribs bilaterally (arrow). **C** Lumbar spine demonstrates lumbar gibbus centered at L1 with hypoplasia (arrow). **E** Scaphocephaly, enlarged image of a J-shaped sella turcica from a lateral radiograph of the skull. **F** Radiograph of the hand demonstrates bullet-shaped phalanges and widened metacarpals pointed proximally. **D** and **G** Long Bones showed widened diaphysis and cortical thinning. **A** and **D** Pelvis demonstrates an abnormally formed pelvis with rounded or flared iliac wings

Minimal changes in the overall structure of the protein were observed for Ser633Leu or Ser633Trp variants, compared to the WT IDUA structure (Fig. 3A). Root-mean-square displacement (RMSD) values for the C-alpha atoms for Ser633Leu mutant after optimization substitution was 1.58 Å and 1.6 Å for Ser633Trp, compared with atoms in the WT structure (PDB: 3W81), agreeing with previous reports [18]. The RMSD is an indication of a change in a protein structure with respect to the initial position of atoms. A large RMSD means that the protein has undergone large structural changes. In the regions surrounding the mutation site, the structures did not show important changes (Fig. 3B). A partial exposition to solvent of the side-chain in the tryptophan variant was observed (39% of total possible area exposition), in contrast to the leucine variant (3.4%) or the serine wild-type residue (0.6%), which are hidden to the solvent. These little differences did not significantly affect the spatial position of neighboring residues (Fig. 3B). Major structural differences between structures occurred in loops that naturally have the largest movements, as judged from B-factors in the crystallographic structure (Fig. 3C).

5.2 Ser633Trp Mutation Modified the Collective Structural Dynamics of IDUA

In order to gain a better understanding of the collective dynamics of each individual structure, we plotted RMSD values for the C-alpha atoms of all structures across each 50-ns trajectory (Fig. 4). RMSD showed that the equilibration was reached more rapidly in the WT and Ser633Leu structures (10 ns approximately) than in the Ser633Trp structure (around of 25 ns), suggesting that serine and leucine amino acids can confer more conformational stability to the IDUA enzyme in contrast to the tryptophan variant.

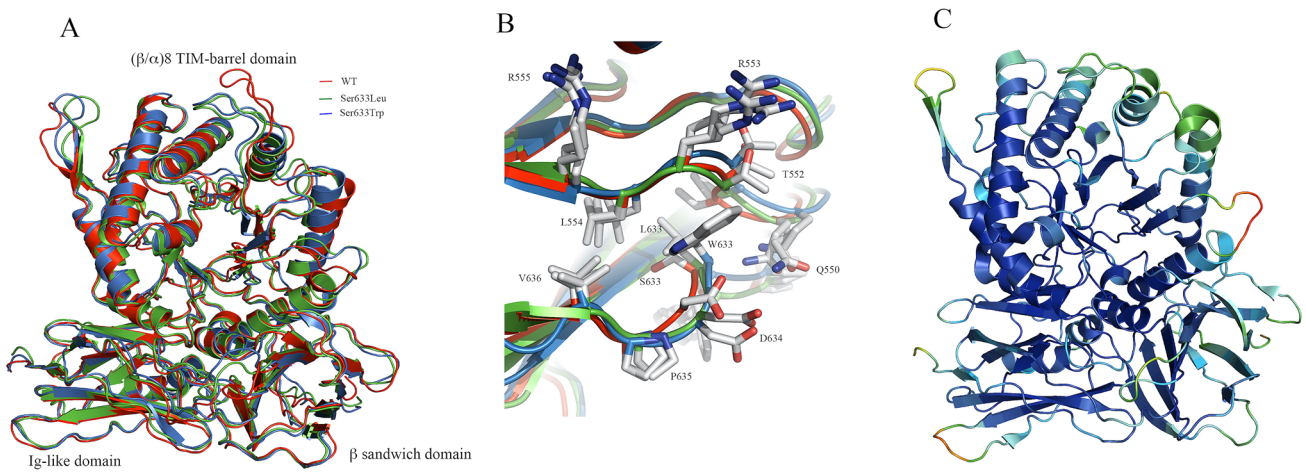

Fig. 3 Effect of mutations on overall structure. **A** Superposition of IDUA WT (red), Ser633Leu (green) and Ser633Trp (blue) final structures. **B** Conformation of side-chain of neighboring amino acids (oxygen, nitrogen and carbon atoms are colored red, blue and light gray, respectively), close to position 633 to IDUA WT (red), Ser633Leu (green) and Ser633Trp (blue). **C** Cartoon representation of the crystal structure of the IDUA (PDB 3W81), colored according to B-factors. B-factor distribution is shown in rainbow colors ranging from blue (low B-factors) to red (high B-factors)

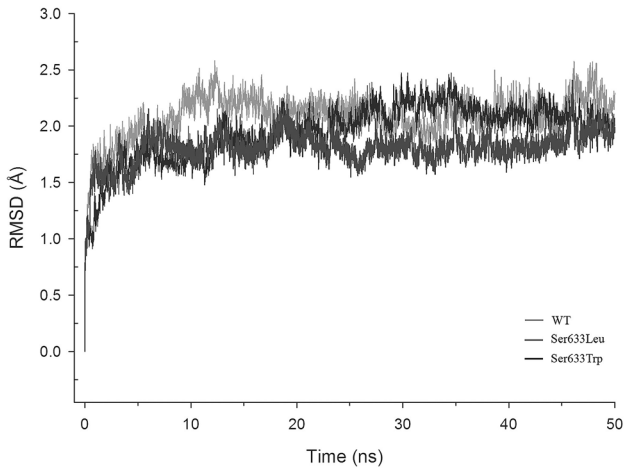

Fig. 4 The RMSD of each simulated IDUA model throughout a 50 ns molecular dynamics simulation. The RMSD of IDUA WT (light grey line) is compared with Ser633Leu (dark grey line) and Ser633Trp (black line) models

Interestingly, equilibration RMSDs through molecular dynamics simulation were greater for WT and Ser633Trp variants (around 2.25 Å), indicating major global structural changes with respect to the initial structure from these models, compared with Ser633Leu variant (1.8 Å). These results suggest different profiles in the molecular dynamics of the three IDUA models that depend on the particular mutation, rather than the effect of the IDUA mutation in the disease phenotype. These results agree with 30-ns molecular dynamics simulations of WT and the relatively high frequency of variants p.Arg89Gln, p.Arg89Trp, and p.Pro533Arg of IDUA. Overall RMSD values of these mutants were greater than for the WT IDUA structure in all cases [19]. However, it is not clear whether those molecular simulations were carried out including the sugars reported in the crystal structure or if these were omitted, which could modify the results of the molecular dynamics.

Another recent report showed that in silico models of human WT-IDUA produced through different online servers yielded structures with greater RMSD values than the crystallographic structure, reinforcing the idea that methodological approaches are determinant to the structural analysis of IDUA [20].

However, it is noteworthy that these mutants are structurally localized around the active site (Arg89), perhaps directly affecting the conformation of the enzyme active site without disturbing the secondary structure. In the case of Pro533 amino-acid, localized in the IDUA β-sandwich domain, it has been reported that it could be involved in the conformation of the TIM barrel of IDUA as well as the spatial positioning of the Asn372-linked N-glycan that contributes to substrate binding, and that may impair catalysis and also possibly the ability of IDUA to bind to its natural substrates [6, 7].

5.3 The Overall Motions Between the Three IDUA Structures are Different

In order to analyze which are the regions that contribute most in the structural dynamic changes in each of the models, which are reflected through the RMSD, principal components analysis (PCA) was carried out. PCA is a widely used approach to extract the slow and functional motions of biomolecules from the MD trajectories. PCA is defined

on the basis of the calculation and diagonalization of the covariance matrix to obtain orthogonal eigenvectors and corresponding eigenvalues. The eigenvectors of the matrix represent the directions of the concerted motions, whereas the eigenvalues of the matrix indicate the magnitude of the motions along the direction [21]. Projections of the first two principal components (eigenvectors) of WT, Ser633Leu and Ser633Trp variants of IDUA, revealed that the WT and Ser633Leu structures explore a different area of conformational space, and sampling that conformational space explored by the Ser633Trp mutant (Fig. 5A) suggested that the presence of the tryptophan residue might change the conformational space of IDUA, and this could be associated to poor enzyme catalysis. The extreme projection of the MD trajectory along eigenvector 1 to each structure is shown in Fig. 5B in the form of sausage plots. The thickness of the sausage plot shows the extent of motion. For WT IDUA, the most significant conformational changes were observed in the regions encompassing residues 102-106, 227-230, 245-253, 372-377, and 443-453, all in the major loops or turns. In the Ser633Leu and Ser633Trp IDUA models, only residues 102-106 have shown similar conformational changes as the WT protein. It is worth highlighting that the residues of loop 372-377 showed minimal changes across the molecular dynamic simulation of the Ser633Leu and Ser633Trp variants. This loop contains the Asn372 that attaches to a high mannose type N-glycan that has been suggested to constitute part of the substrate-binding pocket (Fig. 5D) [7, 22].

Alterations in the conformational dynamics of these residues may impair catalysis and possibly also the binding to its natural substrates. Similar observations have been reported in dihydrofolate reductase from *E coli*, where it was observed that the mutation of an amino acid distant from the catalytic site altered the dynamics of a loop associated with the catalytic function of the enzyme [23].

On the other hand, the loop encompassing residues 243-253 showed a significantly smaller contribution to global displacements in both mutants, compared to those observed in the IDUA WT structure. Amino acid residues that form this loop, and that have not been previously reported as mutation sites associated with the development of MPS I, connect α-helix 9 with β-strand 9 in the TIM-barrel domain. Catalytic function associated to this loop has not been reported for IDUA, but recent reports highlight the effect of the flexibility of non-catalytic loops on enzymatic activity, perturbing enzymatic transformation of substrates and/or binding of these by improving the natural dynamics of global structures. [24].

Interestingly, in the Ser633Trp mutant, the contribution of the Ig-like and β-sandwich domains in the overall

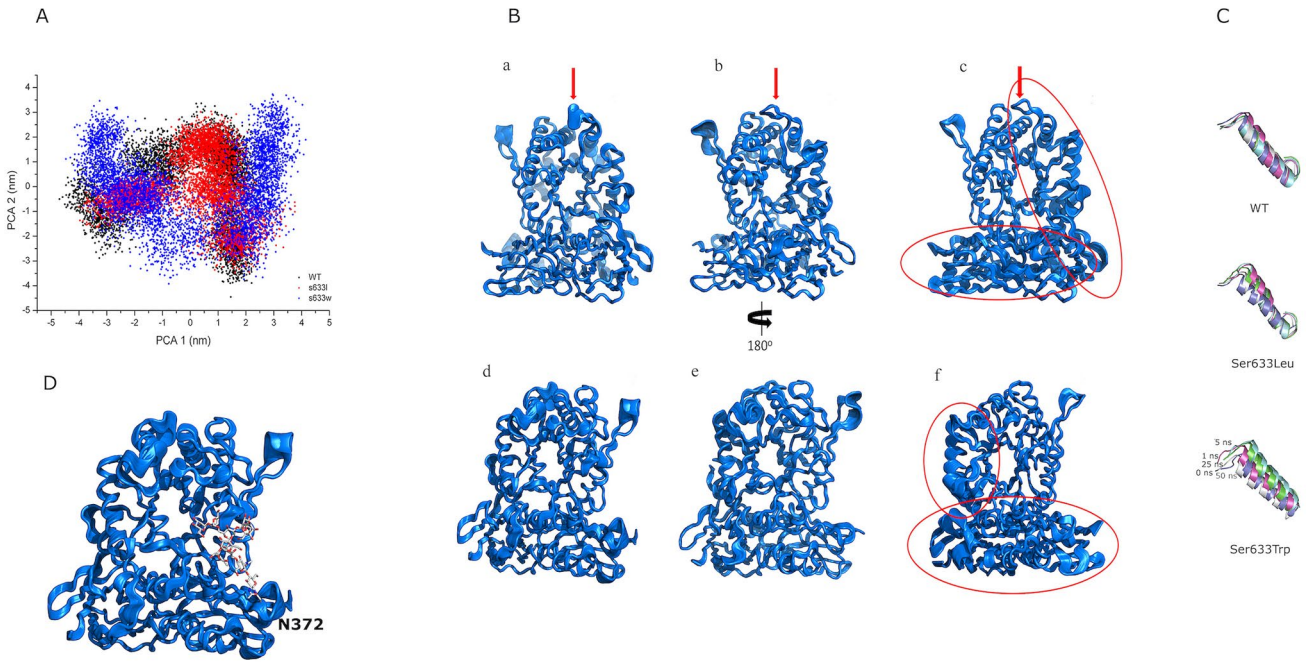

Fig. 5 Principal component analysis of IDUA WT and mutant structures. **A** Projection of trajectory onto first two eigenvectors for IDUA WT (black), Ser633Leu (red) and Ser633Trp (blue). **B** Sausage plots along PC1; the thickness of the plot depicts the extent of motion to IDUA WT (a and d), Ser633Leu (b and e) and Ser633Trp (c and f) structures. The region circled in (c) and (f) shows higher flexibility in Ser633Trp domains. Red arrows highlight the 243-255 loop. **C** Representative snapshot of the alpha-helix 10 extracted at 0, 1, 5, 25, and 50 ns of simulation time. **D** Sausage plots along PC1 for WT IDUA with the N-glycan attached to Asn372 residue indicated as a stick model

dynamics of the mutant, analyzed through the principal component 1, was significantly higher compared to the mutant Ser6333Leu or WT IDUA (Fig. 5B). The increase in the dynamics of these domains seems to affect the dynamic of some regions of the elements that form the TIM barrel. This disturbance is evident in α-helix 10 encompassing residues 269-286, which is close to the active site and attaches Asn372 N-glycan (Fig. 5C), so it could be affecting the dynamics necessary to perform the substrate transformation and therefore the function of the enzyme.

An analysis of residue per residue displacements over the whole simulation period of 50 ns, through Root Mean Square Fluctuations (RMSF), for WT and two mutated IDUA models are presented in Fig. 6A. Regions with large atomic displacements along the trajectory agree with PCA analysis. A significant rise RMSF was observed for residues ~ 100-107, ~ 227-234, ~ 332-343, ~ 369-379, ~ 405-417, and ~ 426-433 in all three models, whereas in WT above average fluctuations are also observed in the loop encompassing residues 269-286. To IDUA mutants, significant rise RMSF was observed for the residues ~ 280-293 to Ser633Leu (localized at the end of α-helix 10) and residues ~ 262-293 (α-helix 10) and ~ 443-452 (loop that connects β-strand 17 with β-strand 18 in the β-sandwich domain) for the Ser633Trp variant, compared whit WT IDUA.

Interestingly, catalytic residues exhibit lower RMSF values in all IDUA structures throughout the simulation. Representative snapshots extracted at 0, 1, 5, 25, and 50 ns confirm that catalytic residues exhibit minor displacements (Fig. 6B). Despite the low values observed in RMSF, the catalytic site shows some distinctly different dynamics between the three models. In the WT and Ser633Leu protein models, larger molecular displacements were observed in the side chains in these residues (Fig. 6B and C), included is the mannose residue (Man 7) that constitutes a part of the substrate-binding pocket [6, 7], compared to that observed for the case of the Ser633Trp mutant (Fig. 6D), suggesting that these little movements may be important for the catalytic activity of the enzyme.

On the other hand, the residues 53 to 67 showed major fluctuations in WT IDUA compared with the mutant models. These amino acids interact with the carbohydrate attached to Asn372 through many polar and nonpolar contacts, principally with Pro54, Leu56 and His58. Dynamic alterations in these residues may impair catalysis and possibly also impair binding to its natural substrates (Fig. 7).

Similarly, the loop formed by residues 243-255 showed greater mobility in the WT protein, compared to the Ser633Leu or Ser633Trp mutants, as judged from the RMSD observed for these residues (Fig. 8A). Snapshots extracted at 0, 1, 5, 25, and 50 ns showed larger displacements of all residues that conform this loop in the WT enzyme (Fig. 8B). This is in contrast with what is observed in both mutant proteins, where this loop is "freezing" (Fig. 8C and D), suggesting a relevant participation of these residues in the enzyme catalysis or in a correct structuration of the catalytic and binding sites.

Amino acid residues that conform this loop have not previously been reported as mutation sites associated with the development of MPS I. Detailed studies of mutations in the Ig-like domain of the IDUA will be necessary to better understand its contribution to the function of this enzyme and possibly will contribute to the design of new therapies against MPS I.

6 Conclusions

Low enzymatic activity observed for p.Ser633Trp variant of the α-L-iduronidase seems to lead to severe mucopolysaccharidosis type I phenotype, possibly associated with a perturbation of the structural dynamics in regions of the enzyme close to the active site or by perturbations of the regions of the enzyme that participate in the binding to the natural substrate that are further away from the active site.

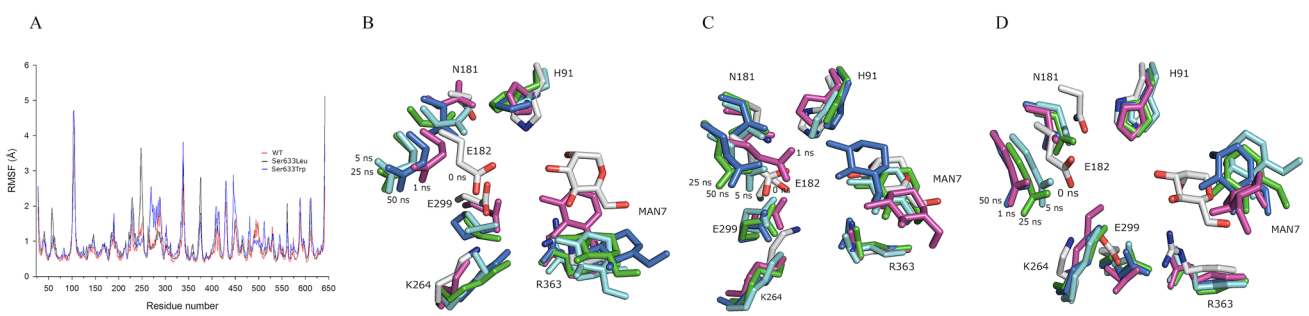

Fig. 6 RMSFs and catalytic site snapshots from MD simulations. **A** RMSF in C-alpha atom coordinates for each residue of WT IDUA (red) Ser633Leu mutant (black) and Ser633Trp mutant (blue), over a 50 ns molecular dynamic simulation trajectory. Representative snapshots of catalytic site residues extracted at 0 (gray), 1 (magenta), 5 (cyan), 25 (green) and 50 (blue) ns form WT (**B**), Ser633Leu (**C**) and Ser663Trp (**D**) IDUA

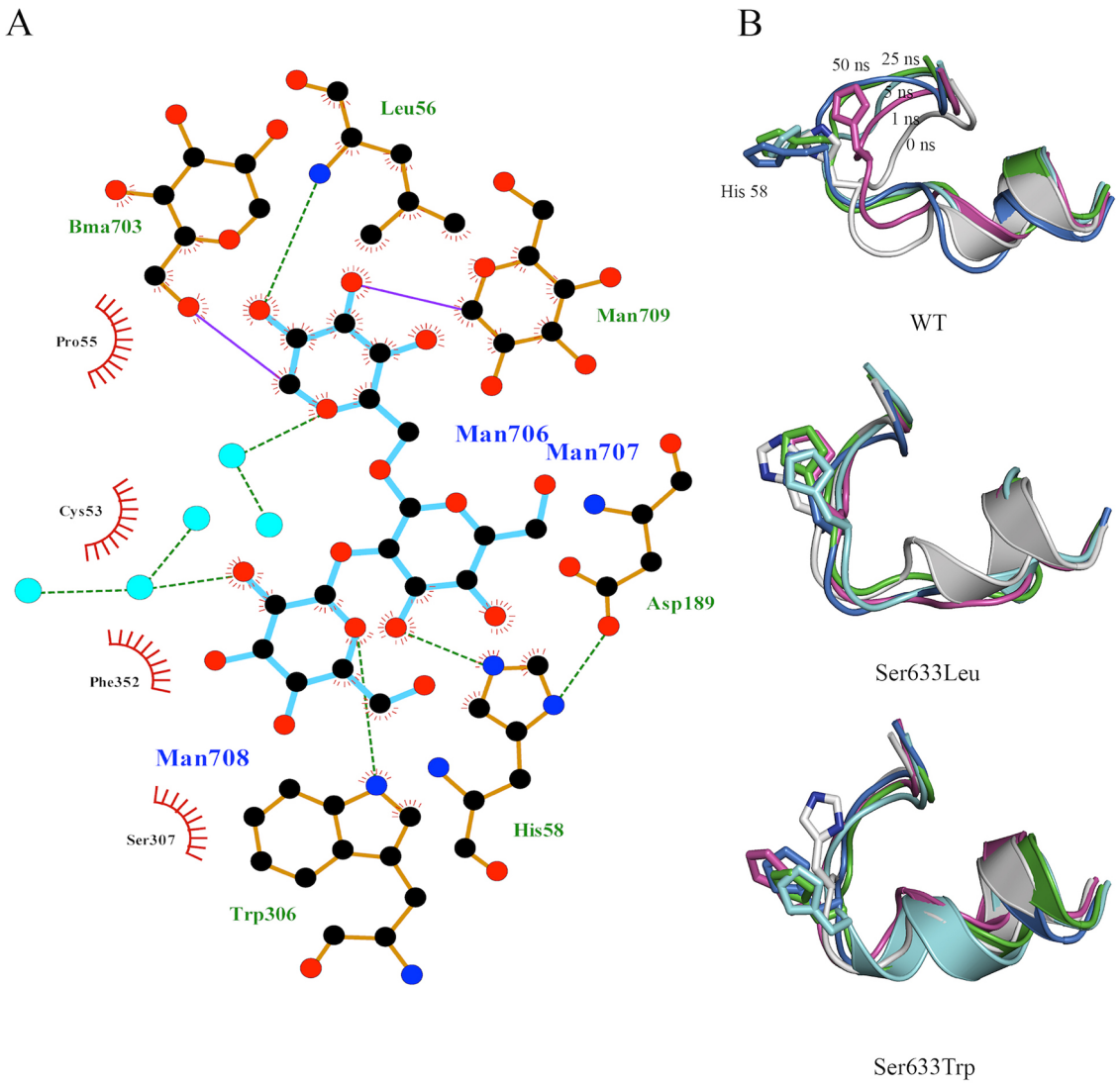

Fig. 7 Details of Asn372 N-glycan-IDUA contacts. **A** Interactions between the N-glycan at Asn372 and IDUA observed in the 3W81 crystal structure, including water molecules (cyan spheres). Polar (green dashed line) and hydrophobic (red arc with spokes) contacts are shown. The figure was prepared with LIGPLOT. **B** Representative snapshots of loop 53-67 extracted at 0 (gray), 1 (magenta), 5 (cyan), 25 (green) and 50 (blue) ns from IDUA WT, Ser633Leu and Ser663Trp

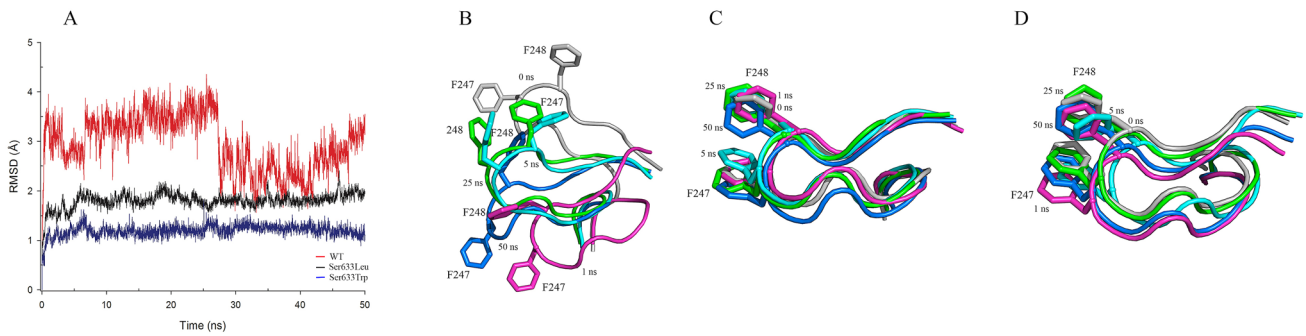

Fig. 8 Loop 233-255-RMSD of each simulated IDUA model throughout a 50 ns molecular dynamics simulation. **A** The RMSD of loop 233-255 of IDUA WT (red line) is compared with Ser633Leu (black line) and Ser633Trp (blue line) models. Representative snapshots of loop 233-255 extracted at 0 (gray), 1 (magenta), 5 (cyan), 25 (green) and 50 (blue) ns from IDUA WT (**B**), Ser633Leu (**C**) and Ser663Trp (**D**). Phenylalanine 247 and 248 (in sticks representation), are shown as reference

Acknowledgements We thank the SIBE-IPN and EDI-IPN. We thank the Sanofi-Genzyme, México for the molecular and biochemical analysis.

Funding This work was supported, in part, by the SIP-IPN [Grant Nos. 20161388, 20170907 and 20182232].

Compliance with Ethical Standards

Conflict of interest The authors certify that they have no affiliations with or involvement in any organization or entity with any financial or non-financial interest in the subject matter or materials discussed in this manuscript.

Ethics Approval, Consent to Participate and Consent for Publication This study was made after obtaining appropriate informed consent, and the Ethical Committee of Pediatric Hospital of Tacubaya approved this study (code number: 309-010-10-17, April 15, 2017).

References

1. Neufeld EF, Muenzer J (2001) The mucopolysaccharidoses. In: Valle D, Beaudet AL, Vogelstein B, Kinzler KW, Antonarakis SE, Ballabio A, Gibson KM, Mitchell G (eds) The metabolic and molecular bases of inherited disease. McGraw-Hill Medical Publishing Division, New York, pp 3421–3452
2. Beck M, Arn P, Giugliani R, Muenzer J, Okuyama T, Taylor J, Fallet S (2014) The natural history of MPS I: global perspectives from the MPS I Registry. Genet Med 10:759–765
3. Scott HS, Guo XH, Hopwood JJ, Morris CP (1992) Structure and sequence of the human alpha-L-iduronidase gene. Genomics 13:1311–1313
4. Scott HS, Anson DS, Orsborn AM, Nelson PV, Clements PR, Morris CP, Hopwood JJ (1991) Human alpha-L-iduronidase: cDNA isolation and expression. Proc Natl Acad Sci USA 88:9695–9699
5. Stenson PD, Mort M, Ball EV, Shaw K, Phillips A, Cooper DN (2014) The human gene mutation database: building a comprehensive mutation repository for clinical and molecular genetics, diagnostic testing and personalized genomic medicine. Hum Genet 133:1–9
6. Bie H, Yin J, He X, Kermode AR, Goddard-Borger ED, Withers SG, James MN (2013) Insights into mucopolysaccharidosis I from the structure and action of α-L-iduronidase. Nat Chem Biol 9:739–745
7. Maita N, Tsukimura T, Taniguchi T, Saito S, Ohno K, Taniguchi H, Sakuraba H (2013) Human α-L-iduronidase uses its own N-glycan as a substrate-binding and catalytic module. Proc Natl Acad Sci USA 110:14628–14633
8. Artola M, Kuo CL, McMahon SA, Oehler V, Hansen T, van der Lienden M, He X et al (2018) New irreversible α-L-Iduronidase inhibitors and activity-based probes. Chemistry 24:19081–19088
9. Terlato NJ, Cox GF (2003) Can mucopolysaccharidosis type I disease severity be predicted based on a patient's genotype? A comprehensive review of the literature. Genet Med 5:286–294
10. Bach G, Moskowitz SM, Tieu PT, Matynia A, Neufeld EF (1993) Molecular Analysis of Hurler Syndrome in Druze and Muslim Arab Patients in Israel: Multiple Allelic Mutations of the IDUA Gene in a Small Geographic Area. Am J Hum Genet 53:330–338
11. Kwak MJ, Huh R, Kim J, Park HD, Cho SY, Jin DK (2016) Report of 5 novel mutations of the α-L-iduronidase gene and comparison of Korean mutations in relation with those of Japan or China in patients with mucopolysaccharidosis I. BMC Med Genet 17:58–62
12. Beesley CE, Meaney CA, Greenland G, Adams V, Vellodi A, Young EP, Winchester BG (2001) Mutational analysis of 85 mucopolysaccharidosis type I families: frequency of known mutations, identification of 17 novel mutations and in vitro expression of missense mutations. Hum Genet 109:503–511
13. Abraham MJ, Murtola T, Schulz R, PaÍl S, Smith JC, Hess B, Lindahl E (2015) GROMACS: high performance molecular simulations through multi-level parallelism from laptops to supercomputers. SoftwareX 1–2:19–25
14. Lee J, Cheng X, Swails JM, Yeom MS, Eastman PK, Lemkul JA et al (2016) CHARMM-GUI input generator for NAMD, GROMACS, AMBER, OpenMM, and CHARMM/OpenMM simulations using the CHARMM36 additive force field. J Chem Theory Comput 12:405–413
15. Aronovich EL, Pan D, Whitley CB (1996) Molecular genetic defect underlying alpha-L-iduronidase pseudodeficiency. Am J Hum Genet 58:75–85
16. Cobos PN, Steglich C, Santer R, Lukacs Z, Gal A (2015) Dried blood spots allow targeted screening to diagnose mucopolysaccharidosis and mucolipidosis. JIMD Rep 15:123–132
17. Ketudat Cairns JR, Keeratichamroen S, Sukcharoen S, Champattanachai V, Ngiwsara L, Lirdprapamongkol K et al (2005) The molecular basis of mucopolysaccharidosis type I in two Thai patients. Southeast Asian J Trop Med Public Health 36:1308–1312
18. Saito S, Ohno K, Maita N, Sakuraba H (2014) Structural and clinical implications of amino acid substitutions in α-L-iduronidase: insight into the basis of mucopolysaccharidosis type I. Mol Genet Metab 111:107–112
19. Tanwar H, Priya Doss CG (2018) An integrated computational framework to assess the mutational landscape of α-L-iduronidase (IDUA) gene. J Cell Biochem 119:555–565
20. Figueiredo DF, Antunes DA, Rigo MM, Mendes MF, Silva JP, Mayer FQ et al (2014) Lessons from molecular modeling human α-L-iduronidase. J Mol Graph Model 54:107–113
21. Maisuradze GG, Liwo A, Scheraga HA (2010) Relation between free energy landscapes of proteins and dynamics. J Chem Theory Comput 6:583–595
22. Jung G, Pabst M, Neumann L, Berger A, Lubec G (2013) Characterization of α-L-Iduronidase (Aldurazyme®) and its complexes. J Proteomics 80:26–33
23. Boehr DD, Schnell JR, McElheny D, Bae SH, Duggan BM, Benkovic SJ, Dyson HJ, Wright PE (2013) A distal mutation perturbs dynamic amino acid networks in dihydrofolate reductase. Biochemistry 52:4605–4619
24. Wang L, Goodey NM, Benkovic SJ, Kohen A (2006) Coordinated effects of distal mutations on environmentally coupled tunneling in dihydrofolate reductase. Proc Natl Acad Sci USA 103:15753–15758